

Evidence of phonon-absorption-assisted electron resonant tunneling in Si/Si_{1-x}Ge_x diodes

Ž. Matutinović-Krstelj, C. W. Liu, X. Xiao, and J. C. Sturm
Department of Electrical Engineering, Princeton University, Princeton, New Jersey 08544

(Received 15 October 1992; accepted 20 December 1992)

We report a study of temperature dependence of electron resonant tunneling diodes in an Si/Si_{1-x}Ge_x material system grown by rapid thermal chemical vapor deposition. Up to four highly symmetric resonances were observed, but the lowest energy resonance has an anomalous temperature behavior, decreasing in strength with decreasing temperature below 140 K and entirely disappearing below 50 K. The temperature behavior and bias position of the resonance are consistent with a model of phonon-absorption-assisted tunneling with a phonon energy of 14 ± 2 meV. The phonon is thought to be an acoustic phonon which promotes Umklapp scattering between the conduction band minima in the emitter and quantum well states.

I. INTRODUCTION

In Si_{1-x}Ge_x heterostructures the resonant tunneling of holes has been extensively studied in recent years,¹⁻³ but the electron resonant tunneling has not received much attention. To the knowledge of the authors there has been just one experimental report of the resonant tunneling of electrons in this material system.⁴ This is mainly due to the energy band configuration, namely the relatively large valence band offset of a strained Si_{1-x}Ge_x layer grown on a Si substrate. To achieve the electron resonant tunneling, a certain offset in the conduction band is needed. This can be accomplished by exploiting a strained Si/relaxed Si_{1-x}Ge_x heterojunction grown on a relaxed Si_{1-y}Ge_y buffer on top of a <100> Si substrate. Such a structure requires a capability of growing high-quality, *n*-type doped, relaxed Si_{1-x}Ge_x layers. In this article we report the fabrication and experimental results of electron resonant tunneling diodes grown by rapid thermal chemical vapor deposition (RTCVD). Up to four symmetric resonant features for both positive and negative biases were observed, but the lowest bias resonance exhibits an anomalous temperature behavior. A model of resonant tunneling by phonon absorption is proposed to explain this temperature dependence.

In these structures, Si layers are subjected to tensile strain. The strain causes splitting of the conduction bands, such that the four valleys along the k_x and k_y axis move up in energy, while the two valleys along the k_z axis (growth direction) move down. The two valleys form the conduction band edge in Si which is actually lower than that of the surrounding SiGe. The conduction band offset is expected to be ~ 200 meV for Si_{0.65}Ge_{0.35}/Si heterojunction, calculated according to the model of Van de Walle and Martin.⁵ The twofold degenerate lowest band in the strained Si has a heavy mass in the z direction ($m_z \approx 0.98$). Due to the large conduction band splitting (~ 230 meV), it is expected that only the heavy electrons will be involved in the tunneling process. The schematic conduction band diagram of the structure at zero bias is shown in Fig. 1.

II. DEVICE FABRICATION AND RESULTS

The structures were grown by RTCVD⁶ on a <100> *n*-type silicon substrate. A 0.5- μm -thick continuously graded Si_{1-x}Ge_x layer was grown at 625 °C up to $x=0.35$. On top of the graded layer a 1- μm -thick, *n*-type doped Si_{0.65}Ge_{0.35} buffer was grown, doped $\approx 7 \times 10^{18} \text{ cm}^{-3}$ using phosphine as the dopant source. The growth was followed by an *in situ* anneal at 800 °C for 1 h, which provided a fully relaxed "substrate" for the double barrier structure. Undoped 175-Å-wide Si spacers were grown to prevent dopant diffusion into the barriers and the well. Si_{0.65}Ge_{0.35} barriers were grown at 625 °C, with the thicknesses varying from 40 to 70 Å on different samples. The silicon quantum well was grown at 700 °C, and its width varied from 20 to 50 Å on different samples. On top of the double barrier structure *n*-type Si_{0.65}Ge_{0.35} ($\approx 0.1 \mu\text{m}$) layer was grown, with the top 300 Å very heavily doped ($\approx 10^{20} \text{ cm}^{-3}$) to provide ohmic contacts. The devices were fabricated by a simple-mesa process. The metal (Ti/Al) was used as a mesa mask and the contacts were annealed for 20 min in forming gas at 350 °C. The mesa sidewalls were not passivated. The device area varied from 60×60 to $130 \times 130 \mu\text{m}^2$.

Symmetric resonant tunneling of electrons for various well and barrier widths was observed. The devices with wider wells exhibit more resonant peaks, as expected, due to lower states in the well, but the resonances are weaker compared to the narrower well devices (25 Å). Up to four positive and four negative highly symmetric resonances have been observed.⁷ The peak-to-valley ratios of 2 were observed for the sharpest resonance at 4.2 K for the devices with the well widths of 25 Å and barrier widths of 60 Å (Fig. 2). The symmetric position of the resonances for positive and negative biases implies symmetric spacer thicknesses, which implies negligible phosphorous segregation at the lower n^+ SiGe/Si interface.

Figure 2 shows typical I - V curves at several different temperatures for a device with well and barrier thicknesses of 25 and 60 Å, respectively. In the I - V curves resonances start to appear at about 225 K (at 240 K in dI/dV curves). At 150 K [labeled (b) in Fig. 2] the two distinct peaks are

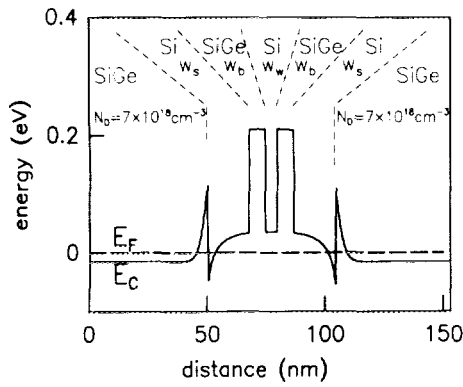


FIG. 1. Schematic conduction band diagram at zero bias. Also shown are the different layers: silicon spacers, $w_s = 175 \text{ \AA}$; $\text{Si}_{0.65}\text{Ge}_{0.35}$ barriers, $w_b = 40\text{--}70 \text{ \AA}$; and Si well, $w_w = 20\text{--}50 \text{ \AA}$. The structure is grown on the top of a graded, $\text{Si}_{0.65}\text{Ge}_{0.35}$ relaxed buffer.

obvious. When the temperature is further decreased the higher bias peak (labeled HE_0) becomes sharper, but the lower one (labeled X) becomes weaker, completely disappearing at low temperatures (d). Devices with different well and barrier widths all qualitatively exhibit the same temperature behavior, except that the number and strength of resonances varies. All of the resonances except the lowest are strongest at 4 K and decrease with an increase in temperature.⁷ The lowest energy resonance is not visible below $T \approx 50 \text{ K}$ (even in dI/dV), but rapidly increases in strength up to 120–140 K, above which it slowly disappears into the increasing background current.

Further evidence of the unusual nature of the lowest energy feature is found by comparing the bias position of the observed resonance to those expected based on the calculated levels in the quantum well. For example, in devices with a 50- \AA well and 70- \AA barriers at 80 K there are four distinct resonances observed in the dI/dV curve at the following (positive and negative) bias positions: 112–120, 162–180, 365–400, and 700–900 mV. For the same device the calculated quantum well energies are 11, 43, 96, and 163 meV. Using a simple first-order model to assign resonant features to the calculated state in the well assuming an

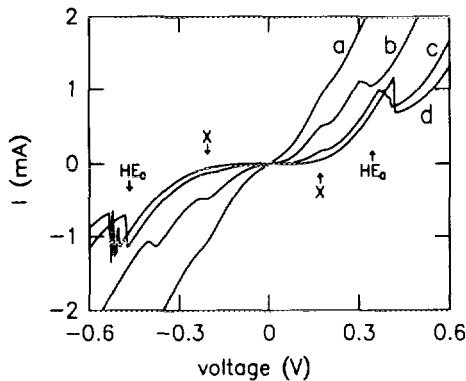


FIG. 2. I - V curves of a device with a 25- \AA well and 60- \AA barriers at various temperatures: (a) 220, (b) 150, (c) 80, (d) 4.2 K.

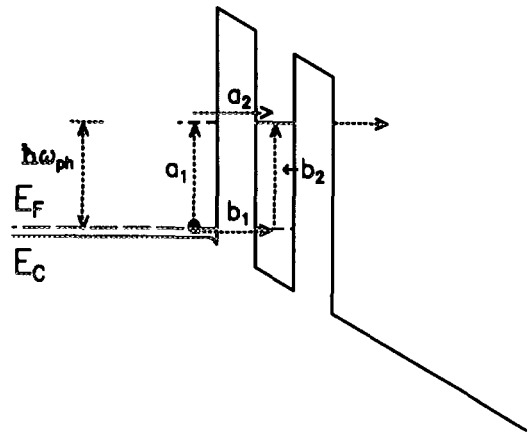


FIG. 3. Schematic diagram of phonon-absorption-assisted tunneling indicating phonon absorption prior to tunneling (path a_1 – a_2) and after tunneling (path b_1 – b_2).

electron effective mass of $0.98 m_0$, no charge buildup in the well, full depletion of the collector spacer, and no voltage drop in the emitter, the expected bias positions are 42, 165, 369, and 627 mV, for the ground state, first, second, and third excited state in the well, respectively (HE_0 – HE_3). The three higher bias resonances are easily associated with the tunneling to the first three excited levels of the quantum well (HE_1 , HE_2 , and HE_3), but the lowest bias resonance does not fit into the model. Since the ground-state energy in the well (HE_0) is calculated to be only 11 meV, tunneling to this state might indeed not be observed, because of too high a Fermi level in the emitter, explaining the absence of the expected 42-mV peak, but not the origin of the 112–120-mV peak. Similar calculations on the samples with different barrier and well widths gave similar results. In devices with narrower wells and hence higher HE_0 states, the HE_0 state was observed, but a lower lying anomalous peak was still also seen (as in the device of Fig. 2). Therefore both the calculation of resonance positions and the temperature behavior suggest a different origin of the lowest energy resonance. To our knowledge, this is the first time that such an anomalous temperature dependence of a resonant peak has been reported. We now propose a phonon-absorption-assisted resonant tunneling model to explain this behavior.

III. PHONON-ABSORPTION-ASSISTED MODEL

There has been evidence of phonon-emission-assisted tunneling in a III-V material system.⁸ In this process an electron can tunnel into the well by emitting an LO phonon near the zone center. Therefore, at higher bias a small replica of the elastic resonance appears in the I - V curve. The voltage difference between the position of the elastic resonance and the phonon replica is related to the LO phonon energy.

We propose a model for the low bias feature involving electron tunneling via phonon absorption, as illustrated in Fig. 3. An electron of energy E in the emitter absorbs a phonon to acquire energy $\hbar\omega_{\text{ph}}$ to tunnel into the well state

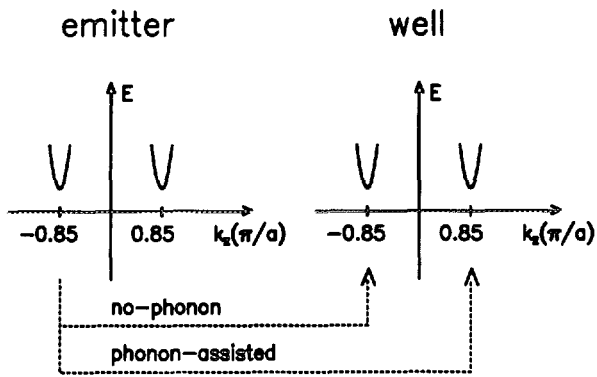


FIG. 4. Schematic diagram illustrating direct and phonon-assisted electron tunneling processes in a SiGe/Si material system. Phonon-assisted process: $\Delta k_z \approx q \approx 2 \times 0.85\pi/a + G \approx 0.3\pi/a$.

$(E + \hbar\omega_{\text{ph}})$. As explained earlier, the conduction band in strained silicon is twofold degenerate, with the heavy electron effective mass along the growth direction (z axis). The two conduction band minima in silicon lie at the Δ point ($k_z \approx \pm 0.85\pi/a$). This enables phonon-assisted scattering from one valley to another, as illustrated in Fig. 4. The transverse momentum is conserved while the absorbed phonon contributes to k_z , with the phonon momentum q equal to $2k_z - G \approx 0.3\pi/a$ (where G is the reciprocal lattice vector). Since the optical phonons have relatively high energies (≈ 62 meV at $q=0$ for Si⁹) we expect acoustic phonons to be involved in this process rather than optical. For a transverse acoustic (TA) phonon in silicon, the energy corresponding to $q=0.3\pi/a$ is ≈ 13 meV.⁹ This would give a peak in the I - V curve corresponding to an energy of 13 meV below the true quantum well state. Given the thicknesses of different layers in the structure, the same first-order model used earlier to relate energy and voltages for a device with 50-Å well and 70-Å barriers predicts a shift in bias position of 50 mV. For the 50-Å well device described earlier, the expected position of the low bias replica of the HE₁ state is then $165 - 50 = 115$ mV, in surprisingly good agreement with the measured biases of 112–120 mV for the anomalous peak. This feature is not observed for higher resonant levels, possibly due to the significant increase in the background current at higher biases.

A careful study of the temperature dependence supports the phonon-absorption hypothesis. The total size of the resonance should be proportional to the number of phonons available (n_{ph}) to be absorbed:

$$I \propto n_{\text{ph}} \propto \frac{1}{e^{\hbar\omega_{\text{ph}}/k_b T} - 1}, \quad (1)$$

where $\hbar\omega_{\text{ph}}$ is the phonon energy. This qualitatively explains the disappearance of the peak at low temperatures. A quantitative analysis was performed by separating the background current by fitting the I - V data at different temperatures to a third-order piecewise-polynomial curve, excluding the data points at the resonance. The edge bias points of the excluded interval at the resonance were manually selected so that the background current fit exhibited

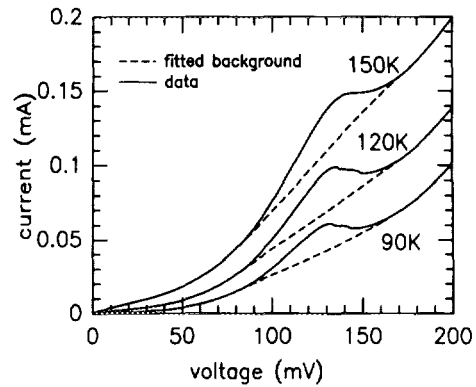


FIG. 5. I - V curves of the lowest energy resonance for a 50-Å well device at three different temperatures.

no resonances or features. The actual data and fitted background I - V curves for a 50-Å well device at three different temperatures are shown in Fig. 5. Figure 6 shows the resulting lowest-bias-resonance strength vs inverse temperature for different devices. Curves (a) and (b) are data for a device with a 25-Å well, for positive and negative biases, and curve (c) is data for a 50-Å well device. The error in the data points due to the background fitting procedure is expected to be less than 10%. The data points were then fitted to Eq. (1) with the phonon energy and a vertical scaling constant as adjustable parameters, yielding the dashed lines in Fig. 6. The resulting phonon energies of 14, 16 and 12 meV for (a), (b), and (c), respectively, are very close to predicted 13 meV for the TA phonon in silicon with $q=0.3\pi/a$, and strongly support the phonon-absorption-assisted model as the origin of the lowest bias resonance.

Any two-step process, such as phonon absorption and tunneling, requires that the system pass through an intermediate state. In the case of the phonon-absorption-assisted tunneling process the electron may become "hot" by absorbing the phonon (step a_1 in Fig. 3) prior to tunneling (step a_2), so that the intermediate state could be a

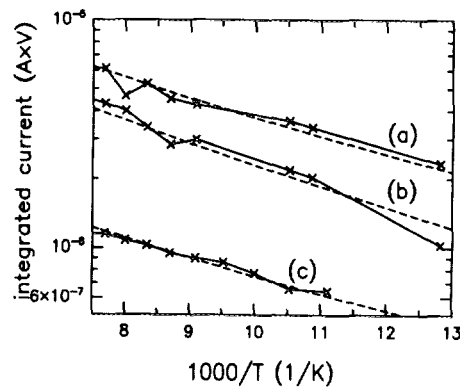


FIG. 6. Integrated tunneling current for the lowest energy resonance vs $1000/T$ for: (a) a 25-Å well device, positive bias, (b) 25-Å well device, negative bias, (c) 50-Å well device. The dashed lines are fits to phonon population curves (a) $\hbar\omega = 14$ meV, (b) $\hbar\omega = 16$ meV, (c) $\hbar\omega = 12$ meV.

true existing state in the conduction band of the emitter with a finite lifetime. This is in contrast to tunneling before the phonon absorption (steps b_1 and b_2 in Fig. 3) or to any path for phonon-emission-assisted tunneling where the intermediate state would be only a "virtual" state. Furthermore, after absorbing a phonon (a_1), an electron will see a substantially lower tunneling barrier height than following the b_1 – b_2 path or any path for phonon emission. Therefore, it is reasonable that transitions through phonon absorption, when allowed by the energy and momentum conservation rules, are much more favorable than phonon-emission related transitions. This could explain why no high-energy replicas corresponding to phonon emission were observed in our samples and why the relative strength of such a resonance is comparable to the true elastic resonance through the level with which it is associated.

A unique feature of the strained Si/Si_{1-x}Ge_x system is that low-energy (and hence plentiful) acoustic phonons may be involved due to the momentum transfer between the degenerate conduction band minima. In a material system with one band minimum, only high-energy zone center optical phonons would be allowed, making such phenomenon much less likely to occur due to a lower number of phonons. That is a possible reason why phonon absorption-assisted features have not been observed for holes in Si/SiGe or in III–V material systems.

IV. CONCLUSIONS

Electron resonant tunneling in a Si/SiGe material system grown by RTCVD has been demonstrated and an anomalous temperature dependence of a low bias resonance has been observed. Both the comparison of observed resonances with the calculated states in the well and the temperature behavior are consistent with a model of phonon-absorption-assisted tunneling. The phonon mediating the process is a TA phonon with momentum $q \approx 0.3\pi/a$ and energy $E_{ph} \approx 14$ meV.

ACKNOWLEDGMENTS

This work was funded by ONR, NSF, and an IBM fellowship award.

¹H. C. Liu, D. Landheer, M. Buchanan, and D. C. Houghton, *Appl. Phys. Lett.* **52**, 1809 (1988).

²S. S. Rhee, J. S. Park, R. P. G. Karunasiri, Q. Ye, and K. L. Wang, *Appl. Phys. Lett.* **53**, 204 (1988).

³U. Gennser, V. P. Kesan, S. S. Iyer, T. J. Bucelot, and E. S. Yang, *J. Vac. Sci. Technol. B* **8**, 210 (1990).

⁴K. Ismail, B. S. Meyerson, and P. J. Wang, *Appl. Phys. Lett.* **59**, 973 (1991).

⁵C. G. Van de Walle and R. M. Martin, *Phys. Rev. B* **34**, 5621 (1986).

⁶J. C. Sturm, P. V. Schwartz, E. J. Prinz, and H. Manoharan, *J. Vac. Sci. Technol. B* **9**, 2011 (1991).

⁷Ž. Matutinović-Krstelj, C. W. Liu, X. Xiao, and J. C. Sturm, *Appl. Phys. Lett.* (submitted).

⁸V. J. Goldman, D. C. Tsui, and J. E. Cunningham, *Phys. Rev. B* **36**, 7635 (1987).

⁹S. M. Sze, *Physics of Semiconductor Devices* (Wiley, New York, 1981).